AVANCES
EN CIENCIAS E INGENIERÍAS
ARTÍCULO/ARTICLE SECCIÓN/SECTION A

Quantum Size Effects in Solid State - Nuclear Magnetic Resonance of metallic particles

Santiago Gangotena[1*]

[1]*Universidad San Francisco de Quito - Vía Interoceánica S/N y Diego de Robles. Cumbayá - Ecuador.*
**Autor principal/Corresponding author, e-mail: sgangotena@usfq.edu.ec*

Editado por/Edited by: Cesar Zambrano, Ph.D.
Recibido/Received: 2015/04/10. Aceptado/Accepted: 2015/05/04.
Publicado en línea/Published on Web: 2015/05/22. Impreso/Printed: 2015/06/01.

Abstract

This work involves the preparation of small metallic particles (of diameters of 200 Å or less) possessing a nuclear spin, I = 1/2, to be used to study quantum size effects (QSE) and surface effects using continuous wave (CW) nuclear magnetic resonance (NMR) techniques. Solvation and pulse methods were used to determine longitudinal relaxation times, T_1, for lead and aluminum powders, where absolute values were found to be 0.45±0.09 and 4.85±0.70 for ^{207}Pb and ^{27}Al, respectively. Approximate values for the Knight shift were also determined (0.168 average for ^{207}Pb and 1.24 for ^{27}Al). In contrast to these findings, ^{109}Ag analysis produced values with high degree of uncertainty. Relaxation times are compared between small particle and bulk measurements, and the relaxation mechanisms and parameters are described.

Keywords. quantum size effects, NMR, spin-lattice relaxation, saturation, surface effects, Knight shift, nuclear spin.

Efectos de Tamaño Cuántico en Estado Sólido - Resonancia Magnética Nuclear de Partículas Metálicas

Resumen

Este artículo involucra la preparación de pequeñas partículas metálicas (diámetros de 200 Å o menores) que poseen un spin nuclear I=1/2 para ser usados en el estudio de los efectos del tamano cuántico (QSE) y efectos de superficie usando técnicas de resonancia magnética nuclear continua. Métodos de solvatación y pulso fueron usados para determinar tiempos de relajación longitudinal, T_1 para polvo de plomo y aluminio, donde valores absolutos de 0.45±0.09 y 4.85±0.70 para ^{207}Pb y ^{27}Al, respectivamente. Valores aproximados para el desplazamiento de Knight fueron también determinados (0.168 para ^{207}Pb y 1.24 para ^{27}Al). En contraste con estas determinaciones, el analisis de ^{109}Ag produjo valores con un mayor grado de incertidumbre. Tiempos de relajamiento fueron comparados con respecto a medidas realizadas en partículas pequeñas y en el material sólido. Finalmente los mecanismos de relajación y sus parámetros son descritos.

Palabras Clave. efecto de tamaño cuántico, NMR, relajación de spin-red, saturación, efectos superficiales, desplazamiento de Knight, spin nuclear.

Introduction

This work presents an NMR study of several metallic powders whose constituent particles have diameters of the order of 200Å or less. Their properties [1–9] can be divided into two areas of study, surface effects and bulk effects. The surface effects arise because of boundary conditions on the electronic wave function at the surface [10]. In a bulk sample it is always assumed that the boundary conditions do not affect the wave function or the electronic energy configuration. The theoretical calculations in the latter case are simplified by the assumption of an infinite solid possessing translational invariance. The invariance is broken by the presence of the surface. The electrons are more localized. The localization affects the average electric and spin densities near the surface. There will also be a redistribution of the ion cores near the surface which changes the potential seen by the almost free electrons of the metal [11]. A reduction of particle size from 1000Åto 100Åincreases the surface to volume ratio by 10. Thus the importance of the surface could mask bulk properties of the small particles.

A more popular approach to the electronic properties of

ISSN 1390-5384

these powders is to look at the discreteness of the energy levels [1–10, 12], a quantum mechanical effect which we expect to be realized in particles of about 200Å or less and at temperatures close to liquid helium [2]. The average energy level spacing δ of the electrons in the small particles is of the order of ϵ_F/N, where ϵ_F, is the Fermi energy and N the number of electrons. For 100 Å particles N is of the order of 10^4 - 10^5.

Several experimental studies [7, 8, 14–25] have been done on very small particles. The measurements are besieged by the small amount of sample available which decreases the signal to noise ratio. One of the methods used to study the electronic properties of these materials is nuclear magnetic resonance (NMR). We have used the continuous wave (CW) technique of NMR to determine the nuclear spin-lattice relaxation time in small metallic particles. Nuclei in metals relax primarily through the hyperfine interaction with conduction electrons given by

$$\mathcal{H} = \frac{8\pi}{3}\gamma_e\gamma_n\hbar^2\vec{I}\cdot\sum_i \vec{s}_i\delta\left(\vec{r}_i\right) \qquad (1)$$

Where γ_e and γ_n are the gyromagnetic ratios of the electron and nucleus respectively, $\vec{s}_i$ and $\vec{I}$ their corresponding spins.

The relaxation mechanism works as follows: when an electron passes close to a nucleus, the nucleus experiences a strong magnetic field, which may induce magnetic transitions between the energy levels of the nucleus, that is, a simultaneous flip of their spins. The energy $\hbar\omega$ required for such a flip is provided by an equal change in the kinetic energy of the electron. The electrons in the metal are governed by the Fermi-Dirac statistics. The average kinetic energy of the electrons is much larger than the thermal energy kT and is of the order of the Fermi energy ϵ_F . Because of the Pauli principle only a fraction kT/ϵ_F at the top of the Fermi distribution contributes to the relaxation process. Even at room temperature this ratio is only of the order of 1% [26].

The spin-lattice relaxation time is found to be of the form [27]

$$\frac{1}{T_1} = a\left|\phi_F\left(0\right)\right|^4\left[\rho\left(\epsilon_F\right)\right]^2 kT \qquad (2)$$

Where a is a constant, $\left|\phi_F\left(0\right)\right|^2$ is the electron density at the nucleus averaged over a spherical Fermi surface and $\rho\left(\epsilon_F\right)$ is the density of states at ϵ_F . We note that the relaxation time is proportional to 1/T. Experimental T_1T values for the metals studied are:

Aluminum 1.8s°K [27]
Lead 29 m°K [28]
Silver 9s°K [29]

From our previous discussion we see that there are two processes which could affect T_1 in small particles: the separation of the energy levels and the physical variations of the surface. We began this work hoping to obtain a variation of T_1 in small particles due to both mechanisms. We reasoned that the redistribution of charges near the surface would cause an increase in the field gradient seen by the nucleus [14, 17] such that the quadrupole mode of relaxation will strongly intervene in metals with nuclear spin I larger than $\frac{1}{2}$. This new interaction would explain the increase in line width [17] and the reduction of T_1 in aluminum and copper [22, 23]. This interaction will not affect metals with $I = \frac{1}{2}$. The quantum size effect (QSE) predicts an increase of the relaxation time in small particles [2]. The increase in the separation of the electronic energy levels will hamper the conservation of energy involved in the spin-flip thus increasing T_1. We expected then, to find such effect in metals like yttrium, lead and silver which have spin $I = \frac{1}{2}$. The QSE could be masked if there is a broadening of the electronic energy levels which, though no longer forming a continuum overlap allowing for energy conservation.

Experimental Methods

Sample Preparation

General considerations

The metal powders were produced by a traditional gas evaporation technique [30, 31]. The bulk metal was evaporated in the presence of an inert gas at pressures of a few Torr [32]. Thin films are produced by evaporation in vacuum. Their characteristics are dependent on the substrate where the atoms fall to form the film. In the production of small particles the gas acts as a cooling agent. Through momentum and kinetic energy exchange upon collisions of the hot metal ions with the lighter inert gas atoms, the former rapidly lose energy and, hence, the chance of forming large particles increases. The evaporated metal forms a cloud of smoke whose shape depends on the type of vessel used for evaporation and on the pressure and the temperature of the inert gas. The smoke diffuses in the chamber coating its walls. The walls then appear to be covered with carbon black. Preliminary runs made with copper in various evaporation chambers showed that the average particle size increased with an increase of the pressure of the gas, with an increase of the temperature of the evaporating metal, and with the distance at which the particles were collected. The inert gas used was helium since heavier inert gases were known to result in large size particles. The cloud of smoke formed is divided in three zones starting at the source which are: nucleation, growth and coagulation. The growth process is described by the equation

$$\frac{dD_i}{dt} = kn(t)$$

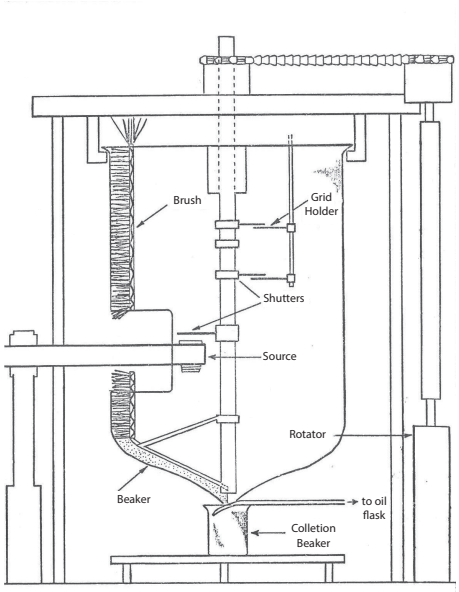

Figure 1: Evaporation chamber inside vacuum system: 400 ml. beaker, boat, brush and collection system

where D_i is the diameter of the i-th particle at time t, n(t) is the concentration of metal ions around the particle i at time t. This law describes well the particle size distribution curves obtained experimentally. The samples to be prepared had to meet the following conditions: (i) the average particle size was to be below 300Å[14]; (ii) oxidation of materials in production, collection and preservation had to be avoided; (iii) the amount of usable sample material had to be such as to yield an observable nuclear resonance signal. The spin $\frac{1}{2}$ metals, with the exception of thallium, have the lowest NMR sensitivities of all materials, a decrease of two orders of magnitude in the signal-to-noise ratio with respect to Aluminum due to their low magnetic moments. In addition the yttrium sample was highly oxidizable and will easily ignite when in contact with traces of air.

Measurements of Particle Size

Procedure

The particle size was determined by study of the x-ray diffraction peaks and by direct measurement of particle diameter from electron microscope photographs. The breadth of the Bragg diffraction lines grow diffuse as the particles or crystallites are less than 10^4 cm [37]. The diameter D of a particle may be determined from the width at half maximum as expressed by the well-known formula [38, 39].

$$D = k\lambda/\beta\cos\theta$$

Where θ is the Bragg angle, λ the wavelength of the radiation and k a constant taken as unity according to usual practice. β is the pure diffraction broadening corrected by the relation

$$\beta^2 = B^2 - b^2$$

Sample		Diameter (Å)	
		X-Ray	**Electron Mic.**
Al	(bulk)	50000	-
	(Small Part.)	220	265 ± 96
Pb	(bulk)	40000	-
	(Small Part.)	150	168 ± 90
Ag	(bulk)	10000	-
	(Small Part.)	108	106 ± 34

Table 1: Average particle diameters. Bulk samples were only measured by the x-ray method. Diameters in electron microscope column were obtained from distribution shown in Figure 3.

where b is the observed breadth of the line produced by a coarse powder giving no line broadening and B is the breadth of the powdered sample. These breadths are all measured at half maximum.

Results

The first material tested was cooper. We found that for a given boat different runs under the same conditions of pressure, temperature and quantity of material being evaporated gave fairly reproducible results. The following typical data was obtained in three successive runs with copper:

Pressure= 0.5 Torr, Temperature= 1110°C,
Evaporation Time= 42 sec,
Average Particle Size(x-ray)=55Å.

Table I gives the x-ray and electron microscope diameters. The histograms of the particle distributions displayed in Figure 3 gave a rough estimate of the distributions Seven samples were collected and preserved with no apparent oxidation. Their coloration remained deep black. Three lead samples were mixed having x-ray diameters of 153, 160, 162 angstroms each. The x-ray diameter of the composite sample is given in Table I and the particle distribution is shown in Figure 3. The silver small particle sample was the result of a single evaporation. The procedure of production is not efficient. Small particles of other spin I=2 materials, mainly silver and thallium, were also produced but were not used extensively as the amount of sample obtained was only marginal or apparent oxidation (color change) had occurred. It is, perhaps, no accident that the main research effort has concentrated on metals such as copper and Aluminum. Their small particles are easier to produce and have a NMR sensitivity 2 orders of magnitude larger than that of spin $\frac{1}{2}$ metals.

NMR Studies

Resonance Equipment

The low signal-to-noise (S/N) ratio of the small metal particle samples made it necessary to use the combination of experimental components shown in Figure 4. A 12 inch Varian 4012-3B electromagnet with a gap of 1.75t't' was used. The current source of the magnet was

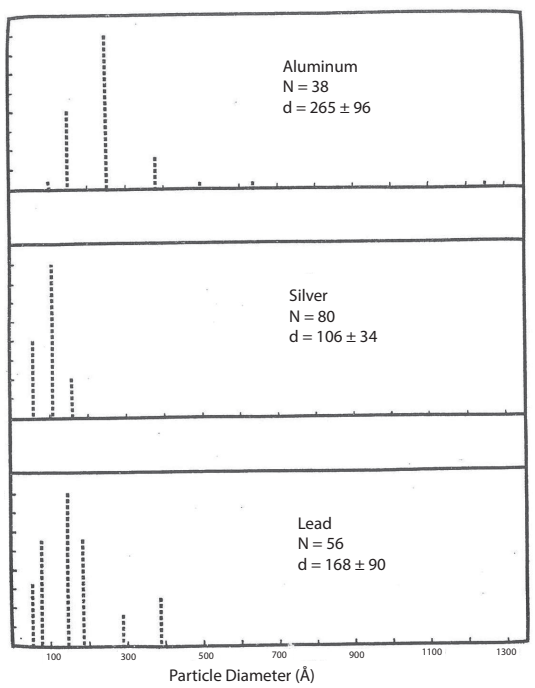

Figure 2: Frequency distribution of particle sizes for N particles from electron miscroscope photographs. Average particle diameters plus or minus one standard deviation are given in each figure.

a Varian 2100-B power supply. The field was varied through resonance with a variable scan ramp voltage from a PAR Boxcar Integrator connected to the sweep input of the power supply. The rf transmitter and receiver of the Varian 4200 NMR spectrometer was used. This is a crossed coil type spectrometer which will receive either the dispersion or absorption signal. The signal was audio-modulated by the V-4250 audio osillator or, directly by the reference signal output of the lock-in through the external input of the V-4250 unit to the coils inside the probe. The modulated signal was detected by a PAR 126 lock-in amplifier adjusted with the PAR 119 preamplifier in the direct mode for test impedance matching. The output of the lock-in, which is proportinal to the derivative of the absorption or dispersion signal was recorded by a HP-7004B x-y recorder and, for initial adjustments by a TeK 546 storage oscilloscope.

Techniques for Determination

An ensemble of nuclear spins in an NMR experiment are well known [40]:

$$\frac{d\vec{M}}{dt} = \gamma\vec{M} \times \vec{H} - \frac{M_z - M_o}{T_1}\hat{z} - \frac{M_x\hat{x} + M_y\hat{y}}{T_2} \quad (3)$$

The first term in this equation describes the motion of the motion of the total nuclear magnetization $\vec{M}$ of free nuclear spins in a dc magnetic field H_o $\hat{z}$ plus an rf field linearly polarized in the z direction, that is

$$H_x = 2H_1 \cos\omega t$$

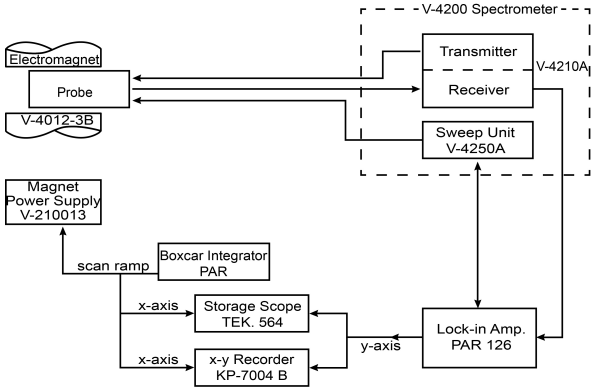

Figure 3: Block diagram of experimental NMR apparatus.

where $2H_1$ is the field measured experimentally. The main contribution to the nuclear spin energy is $H_0 M_z$. The approach of the magnetization towards its equilibrium value M_0 is described by the second term. T_1 is the longitudinal relaxation time. Its value depends on the thermal motion of the atoms and the electronic structure of the sample. The interactions in which the total energy of the spin system does not change, such as spin-spin interactions or magnetic field inhomogeneity affect the transverse components of the magnetization. They are described by the last term. The rate of decay of the transverse components is characterized by a time T_2 known as the transverse relaxation time. In this experiment, the rf field induces transitions among the nuclear energy states. The probability of transition between two states with magnetic quantum numbers m an a mt' is [40, 41].

$$P_{m\to m'} = \frac{1}{2}\gamma^2 H_1^2 \left|< m' \left|I_x\right| m >\right|^2 g(\nu)$$

where $\omega_1 = \gamma H_1, I_x$ is the x-component of the nuclear spin. The shape function g(ν) is a measure of the width of the energy levels distributed about a central frequency ν_o and normalized with respect to frequency by $\int g(\nu)\, d\nu = 1$. The width of the levels is caused by the spin-spin interactions, inhomogeneity of the magnetic field, fluctuating local fields and other T_2 processes. Based on the relaxation times given in the literature for the different bulk samples, we used two different saturation techniques to determine the ratio of the spin-lattice relaxation times in small particles (SP) to bulk (B), T_1^{SP}/T_1^B. We may describe saturation as follows. Assume for simplicity I=1/2. If n denotes the difference in population between the two levels whose populations are Boltzmann distributed we may write the rate equation,

$$\frac{dn}{dt} = {}^{(n_0 - n_1)}/_{T_1}$$

where $n_o = N_\mu H_o/kT$ is the value of n when the spin system is in thermal equilibrium with the lattice. When

radiation is present we add an extra term to account for the net absorption of energy. We obtain

$$\frac{dn}{dt} = {}^{(n_o - n_1)}/_{T_1} - 2nP$$

In the steady state (dn/dt = 0) the solution n_s is

$$\frac{n_s}{n_o} = \left(1 + \frac{1}{2}\gamma^2 H_1^2 T_1 g\left(\nu\right)\right)^{-1}$$

Then the Bloembergen, Purcell and Pound theory and the steady state solution, (slow passage, in Bloch's terminology) of Bloch's equations, Eq.3, are equivalent if we define the quantity T_2 by

$$T_2 \equiv {}^1/_{2g\left(0\right)} \tag{4}$$

giving the main result

$$v = s_o \omega_1 \left(1 + \gamma^2 H_1^2 T_1 T_2\right)^{-1} \tag{5}$$

for the component of the magnetization in quadrature with H_1 [43]. v is called the absorption signal, because it is proportional to the power absorbed by the sample. The dependence of v on H_1 permits us to determine T_1 from the saturation curve of v or the derivative of v [44]. The signal is a maximum when

$$\gamma^2 H_1^2 T_1 T_2 = 1 \tag{6}$$

and decreases at higher fields.

The method of detection used was described in the previous section. The lock-in technique gives a signal proportional to the first derivative of the signal. Redfield(44) has confirmed the validity of the progressive saturation method for the determination of T_1 when the integrated absorption derivative is plotted against H_1 even when fast modulation is being used, that is , when the steady state or slow passage contribution is not fulfilled. For slow passage we must have

$$\omega_m T_1 \ll 1 \tag{7}$$

where $\omega_m = 2\pi\nu_m$ is the modulation frequency. This condition implies that the spin packets must be able to relax between successive modulation cycles. A second condition for slow passage is that the amplitude of modulation H_m, should be smaller than the line width. In solids it is difficult to avoid modulation effects since the relaxation times are of the order of 10msec or greater which would require modulation frequencies of the order of 10 Hz or less. These frequencies are not used experimentally because of noise and stability problems [44]. We found that the S/N ratio increased for $\omega_m <$ $1/T_1$ and less rapidly for $\omega_m >$ $1/T_1$. The signal saturated with an increase of reaching a maximum about the point ω_m $1/T_1$. If the peak-to-peak absorption derivative is plotted against H_1 the signal saturates at a higher field than the peak amplitude of the absorption signal, but the maximum, we also found [42] is sharper in the former case reducing the S/N ratio in a comparative study of relaxation times. However, Eq.5 does not predict the correct saturation behaviour of the dispersion signal [44]. Because of the low S/N ratio of some samples we decided to measure using the derivative of the dispersion signal u (the real component of the complex susceptibility) using a saturation theory developed by Goldman [45]. He obtained a lock-in dispersion signal which saturates normally, that is, the maximum occurs when $\gamma^2 H_1^2 T_1 T_2 = 1$. The signal at the center of the line can be written as

$$u' = u'_o \omega 1 \left(1 + \frac{1}{2}\gamma^2 H_1^2 T_1 g\left(0\right)\right)^{-1} \tag{8}$$

The passage conditions are:

1)

$$H_m \ll \Delta H$$

modulation amplitude less than line width

2)

$${}^1/_{\omega_m} \ll T_1$$

where $\omega_m = 2\pi\nu_m$

3)

$$\omega_m \ll {}^1/_{T_2} \tag{9}$$

4)

$$\omega_m^2 \ll \omega_m^2 T_1$$

5)

$$\int_{-\infty}^{\infty} g\left(\nu\right) d\nu = 1$$

The progressive saturation method requires a knowledge of H_1 and T_2. H_1 can be measured by the rotary saturation or the double resonance method described later. T_2 can be determined from Eq.4 with

$$g\left(0\right) = 2\pi \frac{s\left(0\right)}{\int s\left(\nu\right) d\nu} \tag{10}$$

where s(0) is the experimental shape function at low H_1 field. This definition of T_2 involves the integration of the experimental derivative obtained by lock-in detection (to find s(0)) and further integration to obtain the area under the absorption curve. To focus on the relative values of the relaxation times [46, 47],

$$T_2 \propto {}^{1}/_{\Delta H_{pp}} \tag{11}$$

Sample Preparation and Suspension

A total of 8 samples were used. The Aluminum bulk and small particles were immersed in heptanol. The container was a regular glass test tube. T_1 was measured at room temperature (300°K). The lead samples were also immersed in heptanol. These measurements were taken at liquid nitrogen (77°K) temperature in a liter dewar. The material was placed inside flat 3x6mm glass tubes closed with plastic cap fitted with an o ring. The bulk and small particle silver samples were placed in flat bottom glass tubes to increase the S/N ratio and studied at room temperature. At 77°K too many microphonics from the boiling of the liquid nitrogen were obtained which could not the reduced by fastening the sample tube securely in the dewar or feeding helium gas to the upper section of the liquid nitrogen level above the sample. The yttrium samples were immersed in octoil. They were kept in capped test tubes in a nitrogen atmosphere. We could not find a signal from the yttrium small particles after mixing the powders from 3 separate evaporations. We were able to obtain the dispersion saturation curve for yttrium bulk but we could not find the absorption signal [48, 49].

Theory and Summary of Published Data

We shall consider the research done to date and the ideas proposed concerning the properties of small metal particles under two main headings: the quantum size effect (QSE) as proposed by Kubo [2], and the surface effect [14, 17].

The Quantum Size Effect

Theoretical Considerations

The boundary conditions on the electronic wave function in very small particles give rise to a discrete spectrum of the electronic energy levels. In the free electron approximation to metals the density of states at the Fermi energy ϵ_F is given by

$$\rho\left(\epsilon_F\right) = {}^{3N}/_{4\epsilon_F} \tag{12}$$

where N is the number of electrons in the particle. The average level spacing is defined by

$$\delta = {}^{1}/_{\epsilon_F} \tag{13}$$

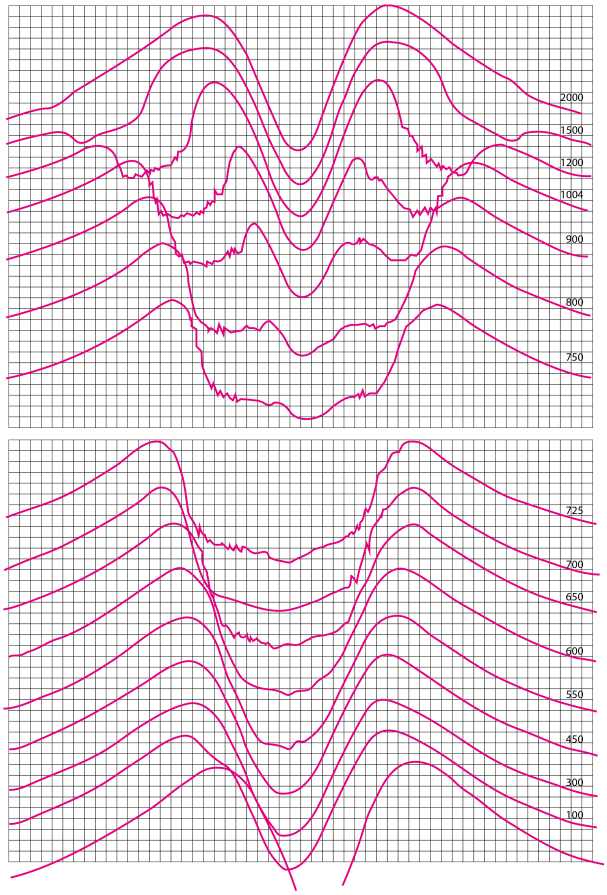

Figure 4: Typical data in rotary saturation experiment: dispersion signal of protons in water heavily doped with manganese ions as a function of audiofrequency.

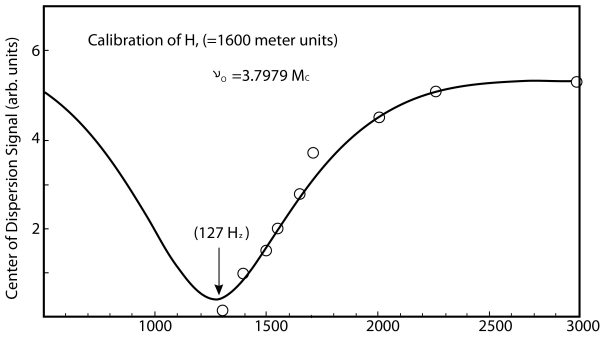

Figure 5: Rotary saturation of protons in water doped with manganese ions. The minimum of the curve occurs at $\nu_a = \gamma H_1/2\pi$. H1 is 0.30 gauss. Fig. 5 showa typical data at differente H_1 setting.

The separation of the energy levels will become apparent when the level spacing is of the order of or less than relevant energies such as the electronic Zeeman energy μ_BH, the nuclear Zeeman energy μ_NH (Table II) and the thermal energy kT. The QSE will then be expected to drastically change (i) the static thermodynamic properties of small particles as determined by the statistical distribution of electrons in the discrete levels and, (ii) dynamical processes as, for example, nuclear relaxation in which nuclear Zeeman energy is exchanged via direct nuclear-electron coupling with the conduction elec-

	Temperature (NMR) T (°K)	**Diameter d(Å)**	**Fermi Energy ϵ_F (ev)**	**Level Spacing δ (ev)**	**Zeeman (Nuclear) $\hbar\omega_n$ (ev)**	**Zeeman (Electron) $\hbar\omega_e$ (ev)**	**Relax. Time (Electron) τ (sec)**	**Broadening ΔE (ev)**
Al^{27}	300	220	11.7	$3.4x10^{-5}$	$1.6x10^{-8}_{(a)}$	$4.0x10^{-5}_{(a)}$	$4.3x10^{-10}_{(c)}$	$1.5x10^{-6}$
Pb^{207}	77	150	9.47	$1.8x10^{-5}$	$1.6x10^{-8}_{(b)}$	$4.0x10^{-5}_{(a)}$		
Ag^{109}	300	108	5.49	$1.9x10^{-5}$	$1.0x10^{8}_{(b)}$	$1.3x10^{-5}_{(b)}$	$8.6x10^{-12}_{(d)}$	$7.6x10^{-5}$

Table 2: Relevant parameters in small particles.

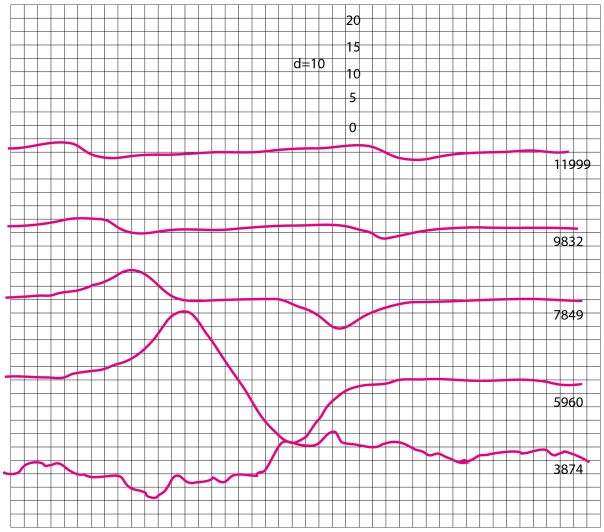

Figure 6: Stdeband signals of protons in water lightly doped with manganese ions. The figures in the right side of each trace are the modulation frequencies.

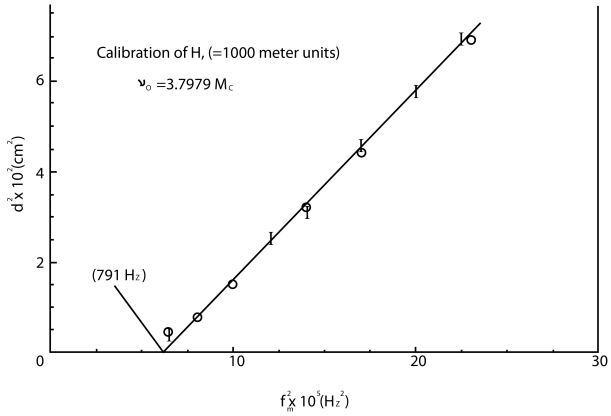

Figure 7: Plot of the square of the distance between resonances in distelled water O nd in heptane with Aluminum small particles I versus modulation frequencies. Intersection of line with horizontal axis is $(\gamma H_1/2\pi)$

tron bath. This process is determined not so much by the statistical distritution as by the large electronic level spacing in small particles which does not allow energy conservation. Table II lists relevant parameters, in the samples studied. The number of electrons in a small particle may be even or odd. The thermodynamic properties are predicted to be different for the two cases. The thermodynamical description is further complicated by the fact that in a given ensemble of particles the energy level distribution in each particle is expected to the different due to their different sizes, shapes and surface irregularities. Three different ensembles were realized depending on the type of symmetry that characterizes the system and on the character of the number of electrons, even or odd [25]. The QSE should disappear in particles where the energy level broadening ΔE is larger than the average spacing δ between levels [52].

Electronic Properties

(a) Kawabata [5] developed an EPR theory in fine particles based on the QSE. The EPR experimental results of Monot et al. [53] in silver at 77°K $\left(kT\ 7\times10^{-3}eV\right)$ are consistent with the theory which predicts a line width of the order $\hbar\omega/\tau_s\delta$ and line shifts toward lower frequencies by the same amount. We noted that the electron spin relaxation time τ_s taken to be proportional to ΔH^{PP}_{-1} is found to be 10^{-8}sec. This value implies that, as far as nuclear relaxation is concerned, the electrons in small particles are at thermal equilibrium as compared with the excited nuclear ensemble. Such is the case in bulk.

(b) The increase of the electronic relaxation time predicted by Kubo and by Holland [54] and realized by the freezing out the electron-phonon interaction in small particles had not been observed in the three metals studied [50, 55, 56] namely, copper: (I=3/2), sodium (I=3) and lithium (I=3/2). The failure to see an increase of τ_s suggests the existence of some type of mechanism which broadens the electron levels enhancing the relaxation process even above the bulk. We briefly mention research in three other areas.

(c) The enhancement of the specific heat in the range of 1.5-15°K in indium and lead small particles due to the low frequency surface-phonon modes has been discussed [8]. The atoms at the surface are less bound than inside atoms and thus can have larger displacements and lower frequencies. The results appeared to be consistent with estimates of the low-frequency cutoffs in the phonon spectrum caused by the QSE. Nonnenmacher [9] explains the enhancement of the specific heat using the asymptotic behaviour of the specific heat formula in the limits of high and low temperature and Kenner and Allen [13] determine a corrected density of states by considering the effect of the surface.

(d) Meier and Wyder [7] found that the magnetization of small indium particles saturates at low fields. The effect cannot be explained using the QSE as developed by Kubo.

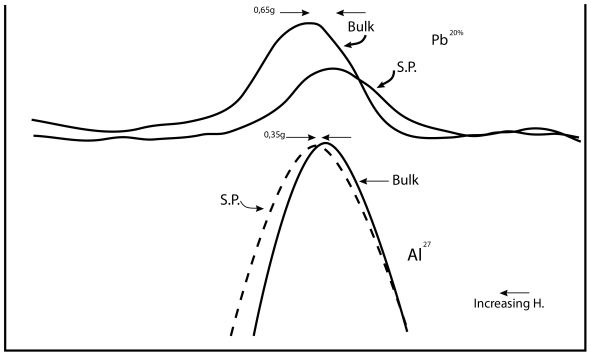

Figure 8: Tracing of dispersion signals in lead and aluminum, bulk and small particles (S.P.), showing a shift in the position of the peak.

NMR Studies

All NMR experiments in small particles have been performed in copper, Aluminum and lithium perhaps because of the large signal-to-noise ratio and relative ease of producing small particles of these metals.

(a) Peak-to-peak line width ΔH_{PP} in Al small particles was independent of temperature in the range of 1.4 - 4.2°K [19].

(b) The intensity of the resonance signal decreased with a decrease in particle size and temperature. Between 1 and 10 °K the intensity is linear on a log-log plot for the two variables.

(c) In particulate, Aluminum T_1 decreases in the range 1.5 - 4.5°K and increases for T < 1.5° K as compared to bulk Aluminum.

(d) T1 in copper was found to decrease between 1 and 4°K [23]. Two components of the relaxation mechanism were found. One was temperature dependent such that T_1T = 1.27sec°K, the bulk value , and the other was temperature independent increasing in magnitude as the particle size decreased.

(e) Line width in Cu done at 1.4 and 4.2°K showed an increase of ΔH_{PP} with increasing magnetic field, decreasing temperature and decreasing particle size [21, 23, 24].

The Surface Effect

Theoretical Considerations

In discussing the QSE no consideration was given to the presence of the surface except for the boundary condition effect on the electronic wave functions. The experimental results seem to indicate that one cannot avoid including this important physical characteristic of small particles which, clearly, is difficult to deal with.

Before discussing the process of relaxation in metals, the Knight shift must be considered [57]. The nuclei in the metal see an extra magnetic field 4Ho due to the polarization of the s-electrons which have a large probability density near the nucleus. This extra field causes

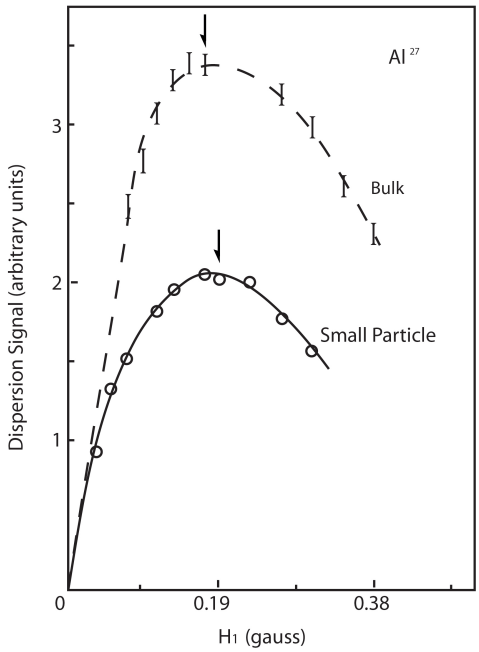

Figure 9: Saturation of aluminum lock-in signal in bulk and small particles. Units are not the same for both curves.

a shift in the resonant positions as compared with the same nuclear species in a non-metallic sample. The electron polarization is temperature independent so the shift is also temperature independent. According for the Knight shift [57],

$$K = {}^{\Delta H_o}/_{H_o} = \frac{8\pi}{3}\chi_e \left|\phi_F(0)\right|^2 \qquad (14)$$

where χ_e is the macroscopic susceptitility per atom per unit volume of the conduction electrons. $|\phi_F(0)|^2$ is the electron probability density at the nucleus for all electronic states at the Fermi surface. If we combine the expression for T_1^{-1} (Eq. 2) with K we obtain the so called Korringa relation [58].

$$K^2 T_1 T = \frac{\hbar\gamma_e^2}{4\pi\gamma_n^2} \qquad (15)$$

The Korringa relation is independent of the electronic structure. The effect of the surface on the NMR results in small particles was first investigated by Charles and Harrison in 1963 [14]. They developed a model based on the picture used by Blandin and Daniel [59] to explain the variations in the Knight shift and troadening of the resonance lines in alloys. Blandin and Daniel find that at low concentrations, the relative variation of the Knight shift is proportional to the amount of dissolved atoms, whereas the broadening increases as the square of the concentration. The effect of introducing a surface is treated by considering a semi-infinite medium and computing the fluctuations $\delta_\rho(x, \epsilon_F)$ in the density of electrons per unit volume per unit energy evaluated at the Fermi energy. The computations are based

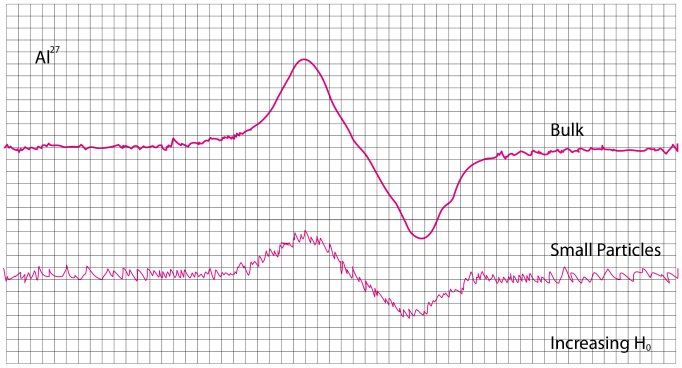

Figure 10: Absorption signals in Aluminum bulk and small particles, H_1 = 38 mgauss. Modulationfrequenxy is 13 Hz. Resonance frequency 3.7979MHz. Sesitivity of lower trace is 5/2 of upper trace. Integration time constant is 10 seconds.

on the free electron model but normalized to the unperturbed density $\rho_o(x, \epsilon_F)$. The nuclei form a lattice at positions x_i which take the values a, 2a, 3a, ... For a semi-infinite medium the authors imposed that the wave function vanished at x=0. The probability density due to a single electron is proportional to $sin^2 k_x x$, where k_x is the x component of the wave number. The charge density averaged over the Fermi surface is

$$\rho(x, \varepsilon_F) = \rho_0 \left(1 - {}^{\sin 2k_F x}/_{2k_F x}\right)$$

where ρ_o is the electron density per unit volume and energy at large distances.

Thus

$$\delta\rho(x, \varepsilon_F) = -\rho_0 {}^{\sin 2k_F x}/_{2k_F x}$$

The Knight shift was then defined as

$$K = \sum_i \delta\rho(x, \epsilon_F) \Big/ \sum_i \rho_0(x, \epsilon_F)$$

and the line brodening as the mean-square deviation of the density evaluated at the nuclei,

$$\Delta = \left\{ \frac{\sum_i |\delta\rho(x, \varepsilon_F)|^2 - |\sum_i \delta\rho(x, \varepsilon_F)|^2}{\sum_i \rho_0(x, \varepsilon_F)} \right\}^{1/2}$$

The sums were calculated over all planes i. Charles and Harrison reasoned that the broadening was caused by the long range electronic charge fluctuations at the surface of the particle which caused a distribution of Knight shifts. These shifts, however, were too small to be observed. The data supported the model; broadening was field dependent indicating that Knight shift effect and the broadening varied inversely with the square root of the particle size.

NMR Studies

(a) Charles and Harrison tested their model of a distribution of Knight shifts in lead small filaments, since the extra broadening of the line $\left\{\Delta H^2 - \Delta H^2\,(bulk)\right\}^{1/2}$ was attributed to this distribution it should vary linearly with the external field. They found a rough linear relationship.

(b) The work in copper by Ido [24] reported a linear relationship between the extra broadening and the field for particle diameters tetween 70 and 600Åand fields below 6 Kgauss. For 70 and 100Åparticles the linear relationship extended to 15 Kgauss. The saturating behaviour of the line width at large fields for larger samples suggested that the absorption lines were composed of two lines; one due to the distribution of Knight shifts and therefore field dependent and the other independent of the field [24].

(c) Ido also found a line width which varied as the inverse square root of the particle diameter, in agreement with the Charles - Harrison surface treatment.

(d) The third effect found was the broadening of the line in Aluminum. Using a 90°-τ-40° pulse sequence and observing an echo Dowley [17] found that the broadening was of quadrupolar origin and not magnetic. The quadrupolar broadening was small (0.35 gauss) but, since it was assumed to be caused by the distribution of Knight shifts the effect should have been small in Aluminum where K=0.16%. The electric field gradient in Aluminum small particles was found to be an order of magnitude larger than in the bulk. The experimental field gradient agreed fortuitously well with the calculated value. The agreement gave strong support to the proposed mechanism of broadening.

(e) We finally discussed the Knight shift measurements at low temperatures. Fujita et al. [19] found that the Knight shift in Aluminum small particles was independent of particle size and temperature. On the other hand, Kobayashi [29] repoted a marked Knight shift change in small particles as a function of size and temperature. The shift approached zero as the temperature was lowered below 4.2°K and as the particle size decreased.

		T °K	ν_o MHz	ΔH_{PP} gauss	g(0) msec	H_1 mgauss	T_1^{exp} msec	T_1 msec	T_1^{SP}/T_1^B	K %	K' %
Al^{27}	B	300	3.7979	8.62±0.10	0.290	171±5	4.85±0.70	$6.00\pm0.04_{(a)}$	0.78±0.14	$0.162_{(c)}$	0.01
	SP			8.35±0.20		190±5			$0.66\pm0.14_{(a)}$	0.172	
Pb^{207}	B	77	3.7979	2.05±0.20	0.28	660±7	0.45±0.09	$0.38_{(b)}$	1.58±0.26	$1.24_{(b)}$	-0.02
	SP			2.54±0.35		584±5				1.26	
Ag^{109}	B	300	2.2900	1.25±0.10		192±12			1.65±0.50		
	SP			1.61±0.20		216±12					

Table 3: Experimental results.

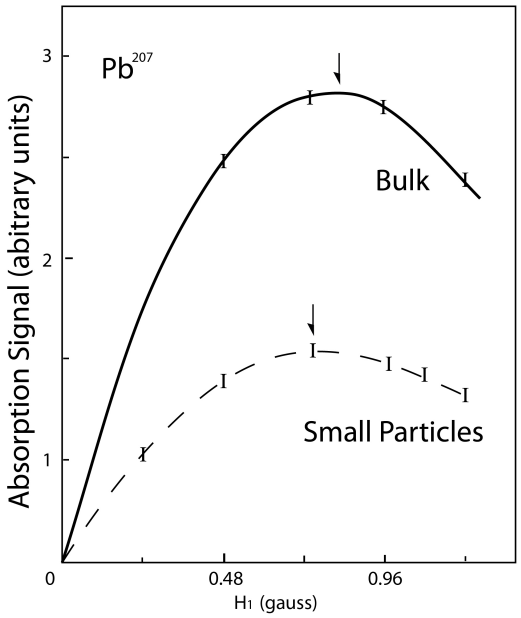

Figure 11: Typical saturation curves in lead bulk and small particles. Ordinate is the peak-to-peak absorption derivative. Units are different in both figures. Arrows indicate maximums, their averages are given in the text.

Both studies were performed in the temperature range between 1.0 and 4.2°K.

Experimental Results

The S/N ratio determined the type of saturation method used to obtain T1 and the ratio of relaxation times between the small particles (SP) and bulk (B) samples, T_1^{SP}/T_1^B. The NMR measurements on the various samples of a specific metal were made under identical experimenta1 conditions to reduce error in the relative values of the relaxation times. Absolute values of T_1 were found only for bulk aluminum and lead using the g (0) value calculated from Eq. 4 and Eq. 10. The ratio of relaxation times vas determined using Eq. 11, from

$$T_1^{SP}/T_1^B = \left(H_1^{SP}/H_1^B\right)^2 \left(\Delta H_{PP}^{SP}/\Delta H_{PP}^B\right) \qquad (16)$$

where H_1 was determined from the maximum of the saturation curves (see Figures 10 and 12) and the average value of H_1 from several curves is given in Table III.

Rough values of the Knight shift were also obtained for aluminum and lead by recording the displacement of the dispersion derivative peaks (see figure 9). Table III gives two values of the Knight shift,

$$K = \left\{\left(H_o - H_o^{SALT}\right)/H_o^{SALT}\right\} 100\% \qquad (17)$$

calculated using the literature values [52] of the bulle shift given by:

Aluminum 0.162% Lead 1.24%

and the measured relative shift defined by

$$K^S = K^{SP} - K^B \qquad (18)$$

Aluminum

The aluminum samples were run at room temperature (300°K) and a resonance frequency $\omega_o/2\pi$ = 3:7979MHz. T_1 was determined by the Goldman method of saturation of the dispersion derivative under fast modulation conditions and slow scan. The frequency of modulation was ν_m = 400Hz and its amplitude H_m = 1:75 gauss.. The scan speed was 0.2 gauss/min with an integration time constant of 10sec. These values satisfy the Goldman conditions (Eq. 9). Figure 10 shows a saturation curve for the two samples. g (0) was determined by integrating the integrated absorption derivative (Eq. 10). The experimental conditions were: ν_m = 13 Hz , H_m = 1:4 gauss, scan speed 1.01 gauss/min, integrating time constant 30 sec, H_1 = 0:019 gauss. The line widths used to determine the ratio TSP $T_2^{SP}/T_2^B = \left(\Delta H_{PP}^B/\Delta H_{PP}^{SP}\right)$ were measured from the curve shown in Figure 11 taken under the same conditions as those used for the g(0) determination except that H_1 = 0:026 gauss. The ratio of relaxation times was compared with the value obtained by Kessemeier [49] in the same samples using the pulse technique (see Table III).

Lead

The lead resonant isotope Pb^{207} occurs with a natural abundance of only 21% and, therefore the best results were obtained by conducting the measurements at liquid nitrogen temperature using the saturation of the absorption method. The resonance frequency was 3.7979 MHz. The modulation ν_m = 80 Hz which satisfies $\omega_m T_1 \approx 1$ and not $\omega_m T_1 << 1$ over the ratio of SP to B $T_1^1 S$ should not be affected. The experimental conditions for recording the atsorption derivatives were

ν_m = 80 Hz , H_m = 1:0 gauss, scan speed 2.9 gauss/min with an integration time constant of 10sec. Figure 12 shows a saturation curve for each sample. We did not plot the absorption peak in order that we could obtain a better relative value of relaxation times avoiding the double integration of the shape functions.

The line widths were determined from Figure 13 under the following conditions: ν_m = 80 Hz , H_m = 1:0 gauss, scan speed 0.24 gauss/min, integration time constant of 100sec and, H_1 = 0:072 gauss.

Silver

Preliminary runs were made in Ag^{109} SP. The line width measurements were taken from Figure 14. Approximate results were obtained by using the Goldman method [46] at ν_o = 2:2900 MHz and room temperature. The saturation experiment was run under the following conditions: ν_m = 80 Hz , H_m = 2:0 gauss which is an order of magnitude larger than the line width given in the literature [53] and therefore does not satisfy the first Goldman condition (Eq.9). The scan speed was 0.18gauss/min with an integration time constant of 100sec. The saturation value of H_1 in bulk and SP is given in Table II. The line width measurements (see Figure 14) were taken with ν_m = 40 Hz , H_m = 1:1 gauss, scan speed 7×10^{-2} gauss/min with an integration time constant of 300sec and H_1 = 0:28 gauss. We note the shift towards high fields of the SP line with respect to the bulk as in the case of lead. No value was quoted as the uncertainty was too large. The data for all three metal samples studied are summarized in Table 3. The uncertainty quoted for the ratio T_1^{SP}/T_1^B was the relative uncertainty $\delta R/R$ calculated from Eq. 16,

$$R = {}^{T_1^{SP}}\!/_{T_1^B} = \left({}^{H_1^{SP}}\!/_{H_1^B}\right)^2 \left({}^{\Delta H_{PP}^{SP}}\!/_{\Delta H_{PP}^B}\right)$$

for the worse case, that is

$$\frac{\delta R}{R} = 2\left(\frac{\delta H_1^B}{H_1^B} + \frac{\delta H_1^{SP}}{H_1^{SP}}\right) + \frac{\delta \Delta H_{PP}^B}{\Delta H_{PP}^B} + \frac{\delta \Delta H_{PP}^{SP}}{\Delta H_{PP}^{SP}}$$

Note that the H_1 values give the largest contributions to the uncertainty.

Interpretation of Data

The discussion of the theoretical and experimental results reported prior to this research points to complex of the description of physical processes in small particles. We divide this section into five topics, relaxation time, line width, Knight shift, broadening of electronic levels and intensity. The latter is included to substantiate our interpretation although we did not take any intensity data.

Spin- Lattice Relaxation Time

We have found, for the first time, an increase of the nuclear spin-lattice relaxation time T_1 in small particles of the spin 1/2 metals lead and silver over their respective bulk values (Table 3). These results are interpreted in terms of the quantum size effect predicted by Kubo. The average energy level spacings δ in small particles become comparable to or exceed the nuclear Zeeman energy and thus the nuclear relaxation via the conduct ion electrons may be inhibited. These results suggested then that the broadening ΔE of the electronic levels was not as large as the average level spacing δ in spin 1/2 particles.

However, the relaxation time T_1 in aluminum (spin I=5/2) small particles decreased. T_1 was measured on the same aluminum sample by the saturation method and by the pulsed technique [60]. The T_1 values obtained agreed within experimental accuracy. The decrease of T1 with decreasing average particle diameters in aluminum at 300°K agrees with the reported resu1ts in a1uminum and copper in the temperature range 1.0-4.2°K for which the broadening ΔE is smaller than δ and which we estimate for our aluminum sample to be one order of magnitude smaller than δ (Table II).

It is our contention that the decrease of the relaxation time in small particles of aluminum as compared to the bulk was caused by the quadrupolar interaction which only exists in materials with nuclear spin larger than 1/2. There are two possible contributions to the relax at ion process via the quadrupolar interaction; one due to the conduction electron density and another due to the ionic charges. The latter couples the nuclear spins to the lattice vibrations and is considered to be negligible in bulk metals [61]. But in small particles it could be enhanced by the increased lattice spacings at the surface and by surface phonons. In this case it was expected the relaxation time to be temperature dependent in contradiction to the temperature independent component of T_1 found in copper [23] in the temperature range 1.0 - 4.2°K. The paramagnetic oxides are suggested to be the cause of the T component through the diffusion process. This temperature behaviour also contradicts the conclusions of Mitchell [62] for relaxation in metals.

To explain the discrepancy between the experimental value of T_1 in aluminum and the larger theoretical value obtained by considering only the contact part of the hyperfine interaction (s- component), the effect of the non-contact part by the addition of a p-wave component to the electron wave function was included and also considered the effect of the quadrupole interaction due to the conduction electron density. It is believed these modes will shorten the relaxation time in aluminum one may write

$$\frac{1}{T_1 T} = \left(\frac{1}{T_1 T}\right)_{HYP(S)} + \left(\frac{1}{T_1 T}\right)_{HYP(P)} + \left(\frac{1}{T_1 T}\right)_{QUAD}$$

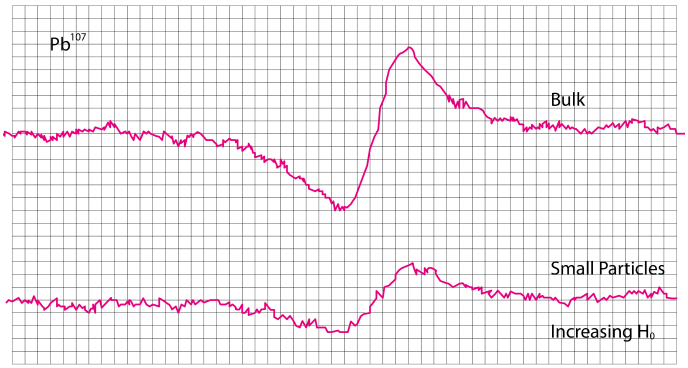

Figure 12: Absorption signals in lead bulk and small particles. H_1 = 0:72 gauss. Modulation frequency is 80 Hz. Resonance frequency3.7979 MHz. integration time constant is 100 sec.

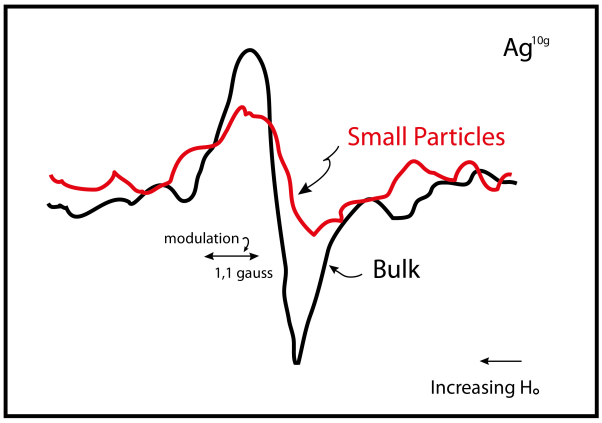

Figure 13: Tracings of absorption signals in silver. H_1 = 0:28 gauss. Modulation frequency is 40 Hz. Resonance frequency is 2.2900 MHz, scan speed 0.07 g/min. Integration time constant is 300 sec.

The two last terms give comparable contributions to the relaxation mechanism, the contact part still being the dominant term. Mitchell concluded that even in aluminum bulk samples at room temperature the non-contact and quadrupole couplings may contribute as much as 20% to the value of the relaxation time. We expect that in aluminum small particles the contribution due to the quadrupolar interaction will certainly be larger since the electric field gradient will increase by as much as one order of magnitude.

Line Width

The introduction of the quadrupolar interaction agrees with Dowleyt's experimental result of quadrupolar broadening in Al small particles. He found that the electric field gradient in Al small particles was 10 times larger than the one produced by strains and dislocations in the bulk. The small broadening (0.35 gauss) reported was explained by the small Knight shift in Al. We note that the line widths reported here are the peak-to-peak values. The values of the line widths in Pb reported by Charles and Harrison are larger than our values by a factor of 2. This suggests that the larger values were caused by modulation broadening.

Knight Shift

We have only rough estimates for the Knight shifts (Table 3) in Al and Pb. The direction of the shifts is in agreement with the Korringa relation; the Knight shift in Al small particles moved towards larger magnetic fields as compared to bulk samples. Recall that $K^2T_1T = constant$; therefore in Al T_1 should decrease as measured. In Pb we found the opposite effect, K decreased suggesting an increase of T_1 with respect to the bulk as measured. Figure 14 shows a displacement of the small particle line towards lower field but no measurement was taken due to the small signal-to-noise ratio. These measurements were taken at 300°K for Al and 77°K for Pb.

Broadening of Electronic Levels

The QSE would be masked if there is a broadening ΔE of the electronic levels which would exceed the average energy level separation δ. There are several mechanisms responsible for broadening of the electronic levels in bulk metallic samples. We may obtain an estimate of ΔE by using the Heisenberg uncertainty relation $\Delta E \geq \hbar/\tau$, which gives a lower limit on ΔE where τ stands for the life-time of the spin state as determined by the various interactions. Elliot [63] pointed out that the dominant interaction contributing to electron spin relaxation is the electron-phonon interaction via the spin-orbit coupling. .He found that the electron spin-lattice relaxation time τ_s could be related to the resistivity relaxation time τ_R by the approximate expression

$$\tau_s \sim {\tau_R}/{(\Delta g)^2} \tag{19}$$

where Δg is the electronic g-shift which is determined by the spin-lattice coupling and the band structure. In metallic particles τ_R can be estimated to be D/v_F , where D and v_F are the diameter of the particle and the Fermi velocity of the electrons (5). The value quoted in Table II was obtained with τ_s $D/v_F\,(\Delta g)^2$. No value could be given for 1ead since τ_s has not been determined. However, Holland showed that the electron-

phonon processes are quenched in small particles below a certain critical diameter D_c. There should be contributions from electron-phonon processes involving a change in the electron energy if $N \geq v_F/\pi v_s$, where v_s is the sound velocity and N the number of unit cells in a crystal diameter. Values obtained for the critical diameters in the metals used in his investigation are:

aluminum 560 Å
lead 1200 Å
silver 730 Å

These values are well above the average particle diameters our samples. The contributions to the relaxation from electron-phonon interactions where the electron energy is unaltered are determined by $D_c < v_s\tau_s$. We estimated for silver: D_c $\tilde{2}$00Å, and for aluminum: D_c $\tilde{4}$00Å. There was no reported value for τ_s in lead, when this document was written.

Multi-phonon processes could be effective in the relaxation since, although being less probable than the one phonon type, their number is much larger. However the one phonon picture is enough to adequately describe resistivity and has been assumed by Holland to describe the relaxation by the Elliot mechanism. In the absence of multi-phonon processes one should therefore expect an increase of the electron relaxation time τ_s [64]. This was not observed. Instead, τ_s decreases.

We finally note that if we use for τ, in the calculation of the uncertainty ΔE, the measured values of τ_s, in the metals for which there is available data we find that in Ag ΔE 10^{-8}eV for D = 10^4 Å(64); in Li and Na ΔE 10^{-7}eV for D = 100Å(55); in Cu ΔE 10^{-7}eV for D = 10^4 Å(55). That is, we obtained a broadening two orders of magnitude smaller than δ.

The preceeding discussion gives only a rough estimate of the level broadening. There is a question of what appropriate τ to use in ΔE $\hbar/\tau$ for small particles. We cannot extrapolate from bulk data as shown by the work of Holland, that is, the electron-single phonon processes is found to be quenched in small particles. Apparently the estimates of τ and the corresponding broadening ΔE given in Table 2 are too high at least for spin 1/2 metals as our results indicate; we found an increase of ΔE. The value of ΔE quoted for aluminum in Table 2 is an order of magnitude smaller than δ and, for the samples used, the electron-single phonon processes are quenched. Therefore, we could expect that this estimate of ΔE is too large. Furthermore, extrapolating to aluminum the values of ΔE determined from the experimental values of τ_s in other metals we could expect a broadening two orders of magnitude smaller than δ. This lends further support to our contention that the decrease of T_1 is of quadrupolar origin and is not masked by the broadening of the electronic levels.

Intensity

The decrease of the intensity of the resonance line with a decrease of the aluminum particle size reported by Fujita et al. was observed by Kessemeier [49]. The existence of a large electric field gradient in the small particles could cause the reduction of line intensity. Fujita observed a decrease of intensity and did not report a broadening of the lines as the particle size decreases. This effect was similar to the second order quadrupole effect seen in alloys [61] where the intensity of the central line decreases as a function of solute concentration and no broadening of the line occurs. If broadening occured the decrease of intensity was assigned to the first order quadrupole effect which appears for field gradients strong enough to broaden the satellites beyond observability and yet not sufficiently strong to split the central line [65]. There is not enough data available for numerical estimates of these effects.

Conclusion

At present there does not exist a detailed dynamical theory which accounts for nuclear relaxation in small metallic particles. such a theory should predict, if not exact values, the dependency of the nuclear relaxation time on characteristic parameters such as the shape of the particles, the type of surface, the surface to volume ratio, the temperature and the value of the nuclear spin. Extrapolating bulk properties to small particles is clearly not permissible. In particular, the Korringa relation for bulk metals must be modified. Comparison between relaxation time calculations and experimental results would further be hampered by scattering in the particle sizes as well as other parameters which would enter in the calculations. To separate the magnetic from the electric contributions to T1 one could check on the ratio $\left(T_{1a}^{-1}/T_{1b}^{-1}\right)_{max} = \gamma_a^2/\gamma_b^2$ of a metal with several isotopes. If the ratio does not hold it would indicate quadrupolar which obeys $\left(T_{1a}^{-1}/T_{1b}^{-1}\right)_{quad} = Q_a^2/Q_b^2$ (61). This research considered only one of the possible parameters involved in the small particle relaxation mechanism, namely, the value of the nuclear spin. An increase in the relaxation time was obtained, a quantum size effect predicted by Kubo [2].

References

[1] Fröhlich, H. 1937. *Physica*, 6: 406.

[2] Kubo, R. 1966. *J. Phys. Soc. Japan*, 17: 975.

[3] Kawabata, A.; Kubo, R. 1966. *J. Phys. Soc. Japan*, 21: 1765.

[4] Gorkov, L.; Eliasberg, G. *Soviet Phys. JETP*, 21: 940.

[5] Kawabata, A. 19670 *J. Phys. Soc. Japan* 29: 902.

[6] Denton, R.; Mühlschlegel, B.; Scalapino, D. 1971. *Phys. Rev. Letters*, 26: 707.

[7] Meier; F.; Wydner, P. 1973. *Phys. Rev. Letters*, 30: 181.

[8] Novotny, V.; Meincke, P. 1973. *Phys. Rev. B*, 8: 4186 (1973).

[9] Nonnenmacher, Th. 1975. *Phys. Letters*, 51A: 213.

[10] Cooper, L.; Hu, S. 1971. "Density of Electron Levels for Small Particles". *Electronic Density of States (U.S. Gov. Printing Office, Washington D.C.)*

[11] Kennard, E.; Waber, J. 1971 "Potential; Charge Density Near the Interface of a Transition Metal". *Electronic Density of States (U.S. Gov. Printing Office, Washington D.C.)*

[12] Kubc, R. 1968. *Comments on S. S. Phys*, 1: 61.

[13] Kenner, V.; Allen, R. 1975. *Phys. Rev. B*, 11: 2858.

[14] Charles, R.; Harrison, H. 1963. *Phys. Rev. Letters*, 11I: 75.

[15] Masuda, Y.; Redfield, A. 1964. *Phys. Rev.*, 133A: 944.

[16] Charlovin, J.; Froidevaux, C.; Taupin, C.; Winter, J. 1966. *S. S. Commun.*, 4: 357.

[17] Dawley, M. 1967. *Phys. Letters*, 24A: 428.

[18] Taupin, C. 1967. *J. Phys. Chem. Solids*, 28: 41.

[19] Fujita, T.; Ohsima, K.; Wada, N.; Sakakibara, T. 1970. *J. Phys. Soc. Japan*, 29: 797.

[20] Kobayashi, S.; Takahashi, T.; Sasaki, W. 1970. *Phys. Letters*, 33A: 429.

[21] Hines, W. 1971 "Low Temperature NMR Study of Small Copper Particles". *Proceedings of the Twelfth International Conference of Low Temperature Physics (Academic Press of Tokyo)*.

[22] Kobayashi, S.; Takahashi, T.; Sasaki, H. 1971. *J. Phys. Soc. Japan*, 31: 1442.

[23] Kobayashi, S.; Takahashi, T.; Sasaki, W. 1972. *J. Phys. Soc. Japan*, 32: 1234.

[24] Ido, M.; Shitukawa, A.; Hoshino, E. 1973. *J. Phys. Soc. Japan*, 34: 556.

[25] Yee, P.; Knight, H. 1975. *Phys. Rev.*, B11: 3261.

[26] Andrew, E. 1955 "Nuclear Magnetic Resonance" *(Cambridge Press, London)*.

[27] Spokas, J.; Slichter, C. 1959. *Phys. Rev.*, 113: 1462.

[28] Asayama, K.; Itoh, J. 1962 *J. Phys. Soc. Japan*, 17: 1065.

[29] Narath, A. 1967. "Nuclear Magnetic Resonance". *Hyperfine Interactions (Academic Press, N.Y.)*.

[30] Beck, O.; Smith, A.; Wheeler, A. 1940. *Proc. Roy. Soc. (London)*, A177: 62.

[31] Beck, O. 1945 *Rev. Mod. Phys.*, 17: 61.

[32] Kimoto, K.; Kamiya, Y.; Nonoyama, M.; Uyeda, R. 1963. *Japan J. Appl. Phys.*, 2: 72.

[33] Yatsuya, S.; Kasukabe, S.; Uyeda, R. 1973. *Japan J. Appl. Phys.*, 122: 1675.

[34] Wada, N. 1967. *Japan J. Appl. Phys.*, 6: 553.

[35] Turkevich, J. "Ultrafine Particles in the Gas Phase". *Fundamental Phenomena in the Material Sciences (Plenum Press, N. Y.)*.

[36] Kuhn, W. 1953. "Introduction in Ultrafine Particles". *(John Wiley, N. Y.)*.

[37] Taylor, A. 1949 "An Introduction to X-Ray Metallography". *Chapman & Hall Ltd., London.*

[38] Alexander, L.; Klug, H. 1950. *J. Appl. Phys.*, 21: 137.

[39] Alexander, L. 1950. *J. Appl. Phys.*, 21: 126.

[40] Bloch, F. 1945. *Phys. Rev.*, 70: 37.

[41] Bloembergen, N.; Purcell, E.; Pound, R. 1948. *Phys. Rev.*, 73: 679.

[42] Goldman, M. 1970. "Spin Temperature NMR in Solids". *Clarendon Press, Oxford*.

[43] Poole, C.; Farach, H. 1971. "Relaxation in Magnetic Resonance". *Academic Press, N. Y.)*

[44] Redfield, A. 1955. *Phys. Rev.*, 98: 1787.

[45] Goldman, M. 1964. *Le Journal de Physique*, 225: 843.

[46] Reference 26, page 105.

[47] Masuda, Y. 1957. *J. Phys. Soc. Japan*, 12: 523.

[48] Narath, A.; Fromhold, T. 1967. *Phys. Letters*, 25A: 49.

[49] Kessemeier, H. *unpublished.*

[50] Anderson, W. 1956. *Phys. Rev.*, 102: 151.

[51] Emsley, J.; Freney, J.; Sutcliffe, L. 1965. "High Resolution NMR Spectroscopy". *(Pergamon Press, Oxford)*, 1.

[52] Keibig, U. 1974. *J. Phys. F: Metal Phys.*, 4: 999.

[53] Monot, R; Narbel, C.; Borel, J. 1974. *Nuevo Cimento*, 19B: 253.

[54] Holland, B. 1967. "Conduction Electron Spin Relaxation in Small Particles". *Magnetic Resonance; Relaxation (North Holla.nd, Amsterdam)*.

[55] Asayama, K.; Oda, Y. 1967. *J. Phys. Soc. Japan*, 21: 937.

[56] Ya, M.; Fetinov, V. 1965. *Soviet Phys. JETP*, 21: 19.

[57] Knight, W. 1956. *S. S. Phys.*, 2: 93.

[58] Korringa, J. 1950. *Physica*, 16: 601.

[59] Blandin, A.; Daniel, E. 1959. *J. Phys. Chem. Solids*, 10: 126.

[60] Poitrenaud, J.; Winter, J. 1964. *J. Phys. Chem. Solids*, 25: 123.

[61] Winter, J. 1971. *Magnetic Resonance in Metals (Clarendon Press. Oxford)*.

[62] Mitchell, A. 1957. *J. Chem. Phys.*, 26: 1714.

[63] Elliot, R. 1954. *Phys. Rev.*, 96: 266.

[64] Smith, M.; Ingram, D. 1962. *Proc. Phys. Soc. (London)*, 80: 139.

[65] Rowland, T. 1961. *Prog. In Materials Science*, 9: 1.